

## Original Research

### Comparison of MnO<sub>2</sub> nanoparticles and microparticles distribution in CNS and muscle and effect on acute pain threshold in rats

Nahid Nosrati<sup>1,2</sup>, Majid Hassanpour-Ezzati<sup>1\*</sup>, Sayyed Zahra Mousavi<sup>2</sup>, Mohammad safi Rahmanifar<sup>1</sup>, Shiva Rezagholiyan<sup>2</sup>

<sup>1</sup>Department of Biology, Basic Sciences School, Shahed University, Tehran, Iran

<sup>2</sup>Department of Pharmacology, Faculty of Pharmaceutical Sciences, Islamic Azad University, Tehran, Iran

## Abstract

**Objective(s):** Recently, applications of MnO<sub>2</sub> nanoparticles and microparticles in industry, pharmacology, and medicine have considerably expanded. Mn distribution and clearance from brain and spinal cord tissue compared with muscle tissue of rats after single subcutaneous injection of nanoparticles and microparticle of MnO<sub>2</sub>. Pain sensory threshold of rat was evaluated as neurologic consequence of the particles on CNS activity of rats.

**Materials and Methods:** Rats divided to control and two experimental groups. Each experimental group received a single subcutaneous injection of MnO<sub>2</sub> nano- and microparticles, respectively. Acute pain thresholds of rats were evaluated by tail immersion method and its weight gain was recorded during these weeks. Samples taken from brain, spinal cord and muscle tissues of rats, once every 2 week for 8 weeks. The tissue Mn level was measured by inductively coupled plasma-mass spectrometry method.

**Results:** Both particles size passed from blood barriers. Unlike brain tissue, manganese completely cleared from spinal tissue after 8 weeks in both groups. Clearance of Mn from muscle tissue is not complete in both of the groups. Weight gain of rats in both groups was slower than control rats. In microparticle group, rats showed progressive analgesia ( $p < 0.05$ ). In nanoparticle groups, rats showed hyperalgesia for first 4 weeks and analgesia during remaining weeks.

**Conclusion:** Change in MnO<sub>2</sub> particles size affect on Mn distribution and clearance from central nervous system. Effect of particles on whole body metabolism varied with its size too. Finally, comparison of pain response of rats among particle treated groups indicates that neurobiological mechanism affected by particles is varied with their size during times after administration.

**Keywords:** Biodistribution, Clearance, MnO<sub>2</sub>, Nanoparticles, Pain

*\*Corresponding author: Majid Hassanpour-Ezzati, Shahed University, Opposite Holy Shrine of Imam Khomeini, Khalij Fars Expressway, Tehran, Iran.*

*Tel: +982151212242, Email: hassanpour@shahed.ac.ir*

*M H E and S Z M equally designed research*

## Introduction

The use of metal oxide nanoparticles is currently developed in all industries; from computer to perfume manufacturing (1). Currently, microparticles and nanoparticles of manganese dioxide (MnO<sub>2</sub>) application in industry, medicine, and pharmacology is increased and therefore human exposure with these particles augmented. The rate of contamination with MnO<sub>2</sub> in environments is higher than other forms of Mn because of MnO<sub>2</sub> use as a substrate for synthesis of other Mn-containing compounds (2). Also, in comparison with other forms of Mn particles, MnO<sub>2</sub> nanoparticles have a higher oxidation power (3). Steel casting and dry battery industries are two major industries in which workers are in contact with MnO<sub>2</sub> nanoparticles. Besides, due to the use of MnO<sub>2</sub> nanoparticles in composition of methylcyclopentadienyl manganese tricarbonyl (MMT) as a gasoline additive, all people that live in big cities are at risk of its toxic effects (4). This nanoparticle is also used in MRI contrast dye (5). Most of the previous information about MnO<sub>2</sub> neurotoxicity is restricted to its chronic effects (6, 7). The high oxidative activity of these particles can cause stimulation of pathological mechanisms and induce adverse effects on cell function, like autophagy, induction of cell apoptosis (8, 9). Indeed, it is reported that changes in particle size from micrometer to nanometer can augment the oxidation power of the particles. This enhancement of oxidative properties of particles increased the probability of undesirable acute effects of nanoparticles on living organisms. The syndrome resulting from chronic exposure to manganese particles in industrial workers is known as manganism and is similar to Parkinson's disease (10). This finding indicates that dopaminergic neurons are one of the main targets of MnO<sub>2</sub> particles in CNS. Recent findings show a relationship between intensity of metal nanoparticles toxicity with their

concentration and size (11). Therefore, the information about size-dependent biodistribution, clearance, and CNS effects of these compounds has practical importance for further applications of these particles (12). Kim and colleagues reported that the application of a certain dose of MnO<sub>2</sub> nanoparticles in a special size does not have any toxic effects on laboratory animals (13). Contrary, others reported that topical administrations of MnO<sub>2</sub> particles with a diameter less than 2 micrometers to monkeys for one day up to 10 months caused wide distribution of Mn in the nervous system and appearance of some neurological symptoms (14). Also, a linear relation between concentration of MnO<sub>2</sub> nanoparticles and production of reactive oxygen substances (ROS) compounds in Hela cells was demonstrated (15). The oxidative power and easily passing of nanoparticles through blood-brain barrier can induce undesirable acute effects on sensory, motor, and cognitive aspects of CNS functions (16). It has been shown that some metal nanoparticles produced some neural dysfunction even after single exposure (17). In contrary, administration of other nanoparticles has no toxic effects on the function of nervous system in animals (18). Therefore, particles on the base of concentration and size have unique neurotoxic effect and must be studied separately. ICP-MS provides a high quality method for measurement of metal particles concentration in various tissues; especially in brain tissues (19). Tail immersion is a method for assessment of animal pain threshold. The efficacy of this method is shown in assessment of pain threshold changes with respect to dopaminergic system manipulation (20). In this research, the Mn level in rat brain, spinal cord, and muscle tissues were measured once 2 weeks for eight weeks by ICP-MS after single subcutaneous injections (100 µg/kg) of MnO<sub>2</sub> micro and nanoparticles for pharmacokinetic comparison of these two particles. Also, body weight gain of rats

during this period was compared between  $\text{MnO}_2$  microparticles and nanoparticles treated groups. Also, pain thresholds of rats in the two groups were determined by tail immersion methods during these weeks for comparison of acute neurological effects of these particles.

## Materials and Methods

### Animals

Male albino Wistar rats (Pasteur's institute, Tehran, Iran) weighing  $150 \pm 5$  g were housed in an air-conditioned colony room on a light/dark cycle ( $21\text{--}23^\circ\text{C}$  and a humidity of 30-40%) and supplied with standard diet and tap water ad libitum. Procedures involving animals and their care were conducted in conformity with the NIH guidelines for the care and use of laboratory animals.

### Selecting the dose

The dose of  $\text{MnO}_2$  nanoparticles and microparticles selected on the basis of You and coworkers report (21). Rats were divided into two groups and treated subcutaneously with solution containing nano- and microparticles of  $\text{MnO}_2$  ( $100 \mu\text{g/kg}$ ) dissolved in saline, respectively. Control rats only received normal saline.  $\text{MnO}_2$  microparticles (Figure 1) used in this research were purchased from MERCK Company, Germany.

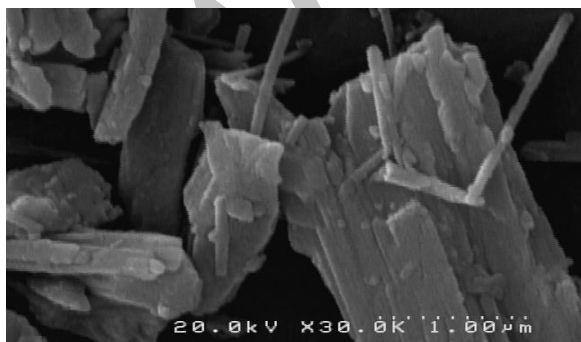


**Figure 1.** A scanning electromicrograph of  $\text{MnO}_2$  microparticles.

### The $\text{MnO}_2$ nanoparticles preparation

$\text{MnO}_2$  nanoparticles were prepared via the hydrothermal procedure proposed by

Zhang et al., with some modification (22). In practice, 20 ml of  $\text{KMnO}_4$  (0.2 mM/lit) were mixed with 16 ml  $\text{MnO}_4$  (0.125 mM/lit) for 5 minutes. The resulting mixture was taken directly into a steel autoclave with Teflon covering and kept for 16 hours at  $160^\circ\text{C}$  and then was cooled at room temperature. The resulting brown product was collected, washed with distilled water and ethanol 3 times, and dried with hot air current  $80^\circ\text{C}$  for 12 hours. The resulting particles were scrutinized by an electron microscope and it was ensured that they were 25 to 85 micrometers in size (Figure 2). Preparing  $\text{MnO}_2$  nanoparticles and microparticles injecting solution.

First, the particles were dissolved in normal saline solution. The prepared solutions were sonicated for 30 minutes before injection.

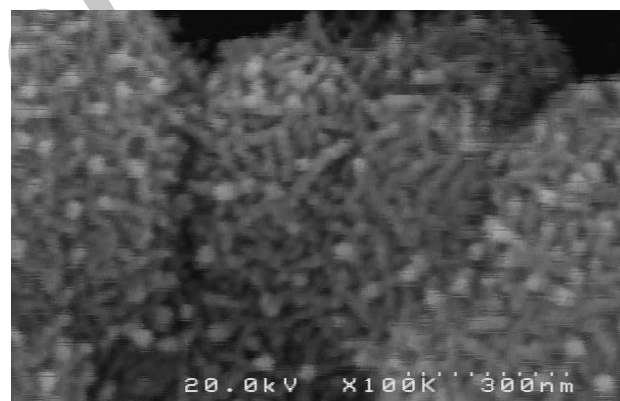


**Figure 2.** Scanning electromicrograph of  $\text{MnO}_2$  nanoparticles.

### Tissue Samples Preparation for ICP/MS measurement

Male Wistar rats ( $140 \pm 10$  g) were used in this experiment. Rats were divided into three groups: control, microparticle, and nanoparticle groups. The experimental groups injected subcutaneously with solution containing  $\text{MnO}_2$  ( $100 \mu\text{g/kg}$ ) microparticles or nanoparticles, respectively.

Control rats received only normal saline. Five rats were chose from each group every two weeks and were deeply anesthetized with diethyl-ether (Merck).

Then, rats scarified and their brains transformed into ice-cold ACSF solution (4°C). The spinal cords of rats were pushed from vertebral canal with perfusion of high-pressure of cold ACSF solution into the vertebral canal. Muscle tissue sample was taken from hind paw of rats (squadriceps femoris).

All samples were frozen with liquid nitrogen after weighting and kept in a -20°C until ICP-MS measurement.

The tissue Mn was extracted by the following procedure: 1/2 gram of each tissue sample was selected and one ml of HNO<sub>3</sub> %63 (Merck, Germany) was added to it (23). Then, the samples were kept for 24 hours at 4°C for complete digestion of the tissues. The digested samples were centrifuged at 4500 rpm for 5 minutes. The upper clear solution was diluted with extra-pure water and the MnO<sub>2</sub> level was measured by ICP-MS (24).

#### ***The ICP-MS measurement of tissue Mn level***

A standard Agilent 7500 ICP-MS, fitted with a crossflow nebulizer and a quartz spray chamber was used throughout (25). Operational parameters are given in Table 1. A solution containing 100 PPM of Mn (Merck) was used as the standard solution.

**Table 1.** Operational parameters of ICP/MS for measurement of Mn level in liver tissue extract.

Parameter	Value	Units
Argon Gas Flow Rates		
Plasma	15.0	L/min
Auxiliary	1.0	L/min
Carrier	1.2	L/min
RF Power	1350	W
Sampling Depth	6.7	mm
Nebulizer	Cross-flow	
Spray Chamber	Double-pass, quartz	
Spray Chamber Temp.	2	°C
Sample Uptake	0.4	ml/min

#### ***Tail immersion test***

The rat pain threshold was assessed using

tail immersion test. After the adaptation, rat tail was immersed in warm water (49°C) and the tail flick response latency (withdrawal response of tail) was observed as the end-point response.

Each experiment was repeated 4 times for each animal with an interval of 2 min and its average was reported. Cut-off time of 25 sec was considered (26, 27).

## **Results**

### ***Tissue Mn level***

The basal level of Mn in brain, spinal cord, and muscle tissues of control rats is 1 (µg/g tissue wet weight). The maximum content of Mn in brain tissue of microparticles group is higher than nanoparticles group.

In MnO<sub>2</sub> microparticles group, Mn level in the brain tissues reached to its maximum level 4 weeks after injection (Figure 3).

Then, the Mn level in this tissue returned to 77.5% its maximal value after 8 weeks. In MnO<sub>2</sub> nanoparticles group, Mn level in brain tissue was reached to its maximum level 2 weeks after injection and its level reduced to 42% its maximum value after 8 weeks. Variation of Mn level in spinal cord tissues during 8 weeks after the injection of particles is shown in Figure 4.

Mn concentration in spinal cord tissues following the injection of MnO<sub>2</sub> microparticles attained its maximum level after 4 weeks, but this time for the nanoparticles receiving group was 2 weeks.

The variation of Mn level in muscle tissues during 8 weeks after the injection of MnO<sub>2</sub> microparticles and nanoparticles is shown in figure 5. In the MnO<sub>2</sub> microparticle groups, Mn level in muscle tissue increase very slowly and reach to a plateau after 2th week.

But in MnO<sub>2</sub> nanoparticle group, the tissue level of Mn increased very fast and reached to high level in second weeks after this particle injection.

But the tissue Mn level quickly decreased to a basal level at 4th week and remained stable till the end of experiment.

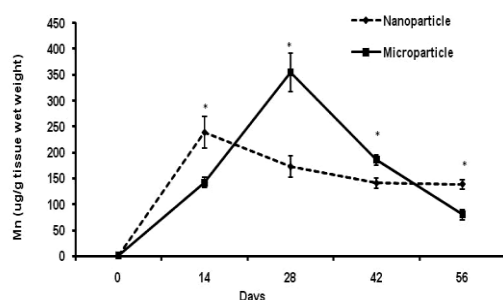


**Figure 3.** Change in Mn level in brain tissues of rat during 8 weeks after single treatment with  $\text{MnO}_2$  (100  $\mu\text{g/kg}$ ) microparticles and nanoparticles. Groups compared by ANOVA and tukey post-test, \* $p < 0.05$  ( $n = 5$ ).

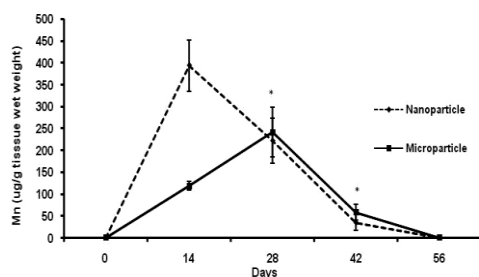


**Figure 4.** Comparison of Mn level in spinal cord tissues of rat ( $n = 5$ ) in  $\text{MnO}_2$  microparticles or nanoparticles (100  $\mu\text{g/kg}$ ) treated groups during 8 weeks. ANOVA and tukey post-test showed a significant ( $p < 0.05$ ) difference in Mn tissues level in between groups.

### Weight gain changes

The rate of weight gain in rats in nanoparticle group in comparison with control rats significantly ( $p < 0.05$ ) reduced during 2th to 4th week after injection (Figure 6).

Weight gain of rats receiving the same dose of microparticles only at the 4th weeks was significantly ( $p < 0.05$ ) lower than control rats (Figure 6).

### Tail immersion measurement of acute pain

The results of tail withdrawal latency of rats in groups during 8 weeks after injections are shown in Figure 7.

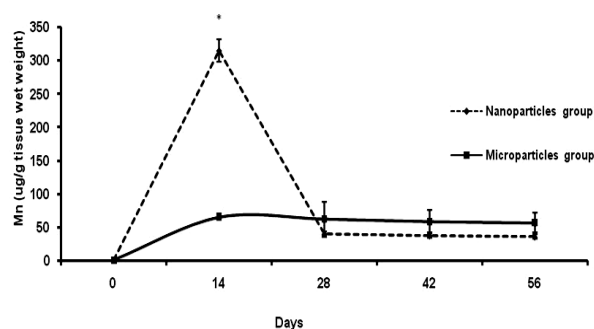


**Figure 5.** Change in Mn level in muscle tissues of rats ( $n = 5$ ) in  $\text{MnO}_2$  microparticles or nanoparticles (100  $\mu\text{g/kg}$ ) groups during 8 weeks after injection. The ANOVA and Tukey post-test show a significant difference ( $p < 0.05$ ) between two groups.

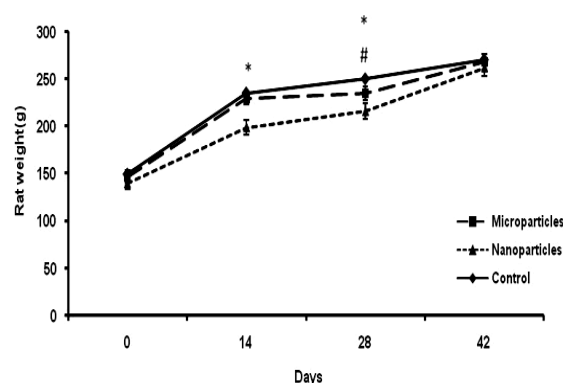


**Figure 6.** Rat weight gain changes during 8 weeks after single subcutaneous injections of  $\text{MnO}_2$  microparticles or nanoparticles (100  $\mu\text{g/kg}$ ) in comparison with control rats ( $n = 5$ ). \*control vs. nanoparticle groups, # control vs. microparticle groups ( $p < 0.05$ ).

The mean tail withdrawal latency of rats before the particles injections was 10 seconds.

The cut-off time was chosen 25-second.

The microparticles injection caused a significant ( $p < 0.05$ ) progressive increase in tail flick latency of rats during 8 weeks. This progressive increase in tail flick latency of rats continued to end of experiment.

The rats treated with  $\text{MnO}_2$  nanoparticles showed a significant ( $p < 0.05$ ) hyperalgesia in the first four weeks after injection and analgesia ( $p < 0.05$ ) during the remaining weeks (Figure 7).

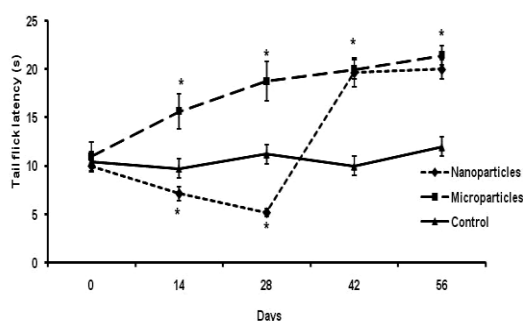


**Figure 7.** Tail flick latency of rats (n=5) following single subcutaneous injections of MnO<sub>2</sub> microparticles or nanoparticles (100 µg/kg) in comparison with the control group. \*Control vs. experimental groups (p<0.05).

## Discussion

Our results showed that basal amount of Mn in normal rat brain is very low. Previous research also has shown presence of very small amount of Mn in brain tissue of human and other animals (28, 29). The Mn level in brain tissue of control rats in this study was proportional with its level in previous studies (30). Measurement of Mn level in brain and spinal cord of rats following administrations of MnO<sub>2</sub> micro and nanoparticles indicate that both types of particles can pass through blood barrier and entered to spinal cord. Previous research has shown Mn can enter and distributed in brain through olfactory bulb (31). It is shown that water soluble and insoluble forms of manganese particles can easily pass through the BBB (32). In this study, Mn clearance rate from brain and spinal cord is not the same for MnO<sub>2</sub> nano- and microparticles receiving groups. The spinal cord tissues were completely cleared from Mn after 8 weeks in both treated groups but brain tissues were not completely cleared from Mn during this time. Previously, it was demonstrated that bioclearance of nanoparticles varies among different tissues; even in tissues have not blood barriers (33).

The Mn clearance rate from brain tissues in microparticle group is faster than nanoparticles group, but Mn clearance rate from spinal cord tissues was the same for

nanoparticles and microparticles treated groups. Sharma and colleagues evaluated permeability range of blood and spinal cord barrier in rats after hyperthermia stimulation with the use of nanoparticles. Their findings suggest that blood-spinal cord barrier permeability variation is more than blood-brain barrier (34).

This report confirms our observation about difference of nanoparticles clearance rates from brain and spinal cord. Previously, it is reported that Mn distributed to all areas of rat brain after intracerebroventricular administration of MnO<sub>2</sub> nanoparticles within three weeks and then concentration of Mn in brain tissue decreased gradually (35, 36).

The time course of this report is equal to time that obtained in our study for reaching of Mn level in brain tissue to maximum value after MnO<sub>2</sub> microparticle administration. Size-dependent differences in tissue bioclearance of particles were shown previously, for example, comparison of fluorescent polystyrene bioclearance microparticles (2 micrometers) with its nanoparticles (200 nanometers) after subconjunctival injections in rats showed that most of nanoparticles disappeared from the periocular tissue during 15 days and only %8 of their initial amount remained in tissues up to 7 days after the injection, but micro particles stayed in the injected tissue for more than two months (37). In nanoparticle group, the Mn slowly accumulated in muscle tissues and reached to plateau at fourth week. In micro particles group, the concentration of Mn in muscle tissue show an initial rise in the second week and then returned to a lower level and stayed at this level till the end of study. A similar situation was demonstrated for clearance of gold nanoparticles from liver and spleen tissues of rats (38).

Thus, the accumulation and clearance pattern of Mn in each tissue special pattern and also changed with particles size. It should be noted that weight gain changes was measured as indicator of general

health status of animals.

The reduction in weight gain of microparticle receiving rats continued for two weeks after the injection, while this effect in nanoparticle-receiving group was longer and continued for four weeks after the injection. Our results show a relation between tissues level of Mn and weight changes of rats. Little information was available about the acute effect of metal oxide nanoparticles on weight changes of animals and most of the researchers have studied the effects of chronic administration of metal oxide particles on the weight changes of animals. Besides, the effect of nanoparticles on weight gain changes of animals varies from one metal oxide nanoparticle to another. For example, intraperitoneal injections of  $\text{TiO}_2$  nanoparticles for 3-month to rats have not any significant effects on its weight gain (39). On the contrary, inhalation of  $\text{Fe}_2\text{O}_3$  nanoparticles significantly affects on rat weight gain (40).

Scientists related these differences in nanoparticles effect on body weight to their oxidative power (41). In support of this statement, it is shown that manganese oxides can cause impaired mitochondrial redox activity (18).  $\text{MnO}_2$  oxidative power is higher than other form of Mn oxides, such as  $\text{Mn}_3\text{O}_4$  (42).

Therefore, our results indicate  $\text{MnO}_2$  particles in both size can influence on the whole body metabolism in rats, moreover the effect of the nanoparticle is slightly higher than the microparticles.

Tail flick latency of rats was evaluated in order to compare effects of the particles on nervous system activity (43).

Scientists previously are used tail immersion latency test for evaluation of analgesia duration after subcutaneously injected nanoparticles (44).

Tail immersion test considered as a model of acute thermal pain (45). Acute pain results from disease, inflammation, or injury to tissue.

Inflammatory processes contribute to nerve cell toxicity (46). Our results

indicate that both size of  $\text{MnO}_2$  particles influenced on pain thresholds of rats.

The administration of microparticles led to a gradual, irreversible increase in the pain thresholds of rats during eight weeks. However, nanoparticles produced biphasic response in rat, initial hyperalgesia for four weeks and late analgesic during last four weeks. On the other hand it has been reported that inhalation of  $\text{MnO}_2$  particles caused changes in the neurochemistry of brain dopaminergic system (47) and severely affect on expression of genes like MAOA, Park2, and SNCA (48). Dopamine also plays a clear role in pain control at the spinal cord level (49, 50) and dysfunctions in this system in spinal cord level can produce deficits in pain sensation (51). Patients with Parkinson's disease showed a progressive hyperalgesia similar to rats treated the  $\text{MnO}_2$  micro particles in our study (52, 53).

As a conclusion we can say that  $\text{MnO}_2$  particles effects on acute pain threshold probably mediated via dopaminergic systems and progressive nature of their effect is similar to Parkinson's disease. As explanation for biphasic effect of  $\text{MnO}_2$  nanoparticles on rat pain responses and according to Wang's finding, a direct relation exists between the level of Mn nanoparticles accumulation in central nervous system and its neurological symptoms (54).

Tissue Mn concentration increased considerably after nanoparticle injection during the first four weeks and then decreased and remained constant during the remaining ones.

Thus, it seems that the neural mechanisms that modulated by  $\text{MnO}_2$  nanoparticles in the first four weeks after injection are different from late-phase mechanisms.

It is shown that manganese ions can interrupt the transmission of stimulatory signals in the nervous system through changes in the activity of calcium channels at pre-synaptic terminals (26).

Also, neuronal evoked potentials of rats showed a significant reduction after long-

term inhalation of MnO<sub>2</sub> nanoparticles (55).

The reduction in activity of descending pain modulation tract can induce hyperalgesia (56).

Thus, it seems that during first four weeks after injection, nanoparticles activate central descending mechanisms that induced hyperalgesia in rats.

Also these mechanisms can mask the MnO<sub>2</sub> nanoparticle analgesic effects in this phase.

But, at the end of first phase and termination of these fast effects, the long term analgesic effect of nanoparticles via effect on dopaminergic system is appeared.

In support of our hypothesis that central dopaminergic system that mediate analgesic effect of MnO<sub>2</sub> nanoparticles, it is reported that depletion of dopaminergic neurons in periaqueductal grey areas of rat brain can induce analgesia (20).

## Conclusions

Administrations of microparticles or nanoparticles of MnO<sub>2</sub> caused Mn accumulation in brain, spinal cord and muscle tissues of rats after single injection for long time. Both sizes of MnO<sub>2</sub> have adverse effects on general metabolism of rats and reduce normal rate of rats weight gain.

The MnO<sub>2</sub> nanoparticle or microparticle has different effect on pain sensation. Probably, change in Mn level in CNS with effect on dopaminergic system mediates its effects on pain modulating systems of rats.

## Acknowledgment

This work was supported by Islamic Azad University, Tehran, Iran and contribution of Shahed University of Iran.

We also thanks from Dr Hassani in ICP/MS lab of Tarbiat Modares University for his helps.

## References

1. Allaker RP, Ren G. Potential impact of nanotechnology on the control of

- infectious diseases. *Trans R Soc Trop Med Hyg.* 2008; 102(1): 1-2.
2. Prasad B, Mondal KK. Environmental impact of manganese due to its leaching from coal fly ash. *J Environ Sci Eng.* 2009; 51(1): 27-32.
3. Najafpour MM, Rahimi F, Aro EM, Lee CH, Allakhverdiev SI. Nano-sized manganese oxides as biomimetic catalysts for water oxidation in artificial photosynthesis: a review. *J R Soc Interface.* 2012; 9(75): 2383-2395.
4. Davis CD, Wolf TL, Greger JL. Varying levels of manganese and iron affect absorption and gut endogenous losses of manganese by rats. *J Nutr.* 1992; 122(6): 1300-1308.
5. Na HB, Lee JH, An K, Park YI, Park M, Lee IS, et al. Development of a T-1 contrast agent for magnetic resonance imaging using MnO nanoparticles. *Angew Chem Int Ed Engl.* 2007; 46(28): 5397-5401.
6. Roels H, Meiers G, Delos M, Ortega I, Lauwerys R, Buchet JP, et al. Lison, Influence of the route of administration and the chemical form (MnCl<sub>2</sub>, MnO<sub>2</sub>) on the absorption and cerebral distribution of manganese in rats. *Arch Toxicol.* 1997; 71(4): 223-230.
7. Oszlanczi G, Vezér T, Sárközi L, Horváth E, Kónya Z, Papp A. Functional neurotoxicity of Mn-containing nanoparticles in rats. *Ecotoxicol Environ Saf.* 2010; 73(8): 2004-2009.
8. Wang SH, Shih YL, Kuo TC, Ko WC, Shih CM. Cadmium toxicity toward autophagy through ROS-activated GSK-3 $\beta$  in mesangial cells. *Toxicol Sci.* 2009; 108(1): 124-131.
9. Nel A, Xia T, Mädler L, Li N. Toxic potential of materials at the nanolevel. *Science.* 2006; 311(5761): 622-627.
10. Bowler RM, Roels HA, Nakagawa S, Drezgic M, Diamond E, Park R, et al. Dose-effect relationships between manganese exposure and neurological, neuropsychological and pulmonary function in confined space bridge welders. *Occup Environ Med.* 2007; 64(3): 167-177.
11. Lison D, Lardot C, Huaux F, Zanetti G, Fubini B. Influence of particle surface area on the toxicity of insoluble manganese dioxide dusts. *Arch Toxicol.* 1997; 71(12): 725-729.
12. Schmidt C, Lautenschlaeger C, Collnot EM, Schumann M, Bojarski C, Schulzke JD, et al. Nano- and microscaled particles for drug targeting to inflamed intestinal



- mucosa-A first in vivo study in human patients. *J Control Release*. 2013; 165(2): 139-145.
13. J Kim JS, Yoon TJ, Yu KN, Kim BG, Park SJ, Kim HW, et al. Toxicity and tissue distribution of magnetic nanoparticles in mice. *Toxicol Sci*. 2006; 89(1): 338-347.
  14. Nishiyama K, Suzuki Y, Fujii N, Yano H, Ohnishi K, Miyai T. Biochemical changes and manganese distribution in monkeys exposed to manganese dioxide dust. *Tokushima J Exp Med*. 1977; 24(3-4): 137-145.
  15. Li Y, Tian X, Lu Z, Yang C, Yang G, Zhou X, et al. Mechanism for  $\alpha$ -MnO<sub>2</sub> nanowire-induced cytotoxicity in Hela Cells. *J Nanosci Nanotechnol*. 2010; 10(1): 397-404.
  16. Muthu MS, Singh S. Targeted nanomedicines: effective treatment modalities for cancer, AIDS and brain disorders. *Nanomedicine (Lond)*. 2009; 4(1): 105-118.
  17. Sarkozy L, Horvath E, Szabo A, Horvath E, Sapi A, Konya Z, et al. Neurotoxic effects of metal oxide nanoparticles on the somatosensory system of rats following subacute intratracheal application. *CEJOEM*. 2008; 14(3): 277-290.
  18. Yang Z, Liu ZW, Allaker RP, Reip P, Oxford J, Ahmad Z, et al. A review of nanoparticle functionality and toxicity on the central nervous system. *J R Soc Interface*. 2010; 7 Suppl 4: S411-422.
  19. Wang J, Chen C, Liu Y, Jiao F, Li W, Lao F, et al. Potential neurological lesion after nasal instillation of TiO<sub>2</sub> nanoparticles in the anatase and rutile crystal phases. *Toxicol Lett*. 2008; 183(1-3): 72-80.
  20. Flores JA, El Banoua F, Galán-Rodríguez B, Fernandez-Espejo E. Opiate antinociception is attenuated following lesion of large dopamine neurons of the periaqueductal grey: critical role for D1 (not D2) dopamine receptors. *Pain*. 2004; 110(1-2): 205-214.
  21. You H, Zhao J, Li L, Yuan J. Effects of MnO<sub>2</sub> Nanoparticles on Liver and Kidney Cells of Rats. *Proceedings of the 5th International Conference on Bioinformatics and Biomedical Engineering (iCBBE) 2011; May 10-12; Wuhan, China*, p. 1-4.
  22. Zhang Y, Yang Y, Zhang Y, Zhang T, Ye M. Heterogeneous oxidation of naproxen in the presence of  $\alpha$ -MnO<sub>2</sub> nanostructures with different morphologies. *Appl. Catal. B*. 2012; 127: 182-189.
  23. Vanhoe H. A review of the capabilities of ICP-MS for trace element analysis in body fluids and tissues. *J Trace Elem Electrolytes Health Dis*. 1993; 7(3): 131-139.
  24. Niazi SB, Littlejohn D, Halls DJ. Rapid partial digestion of biological tissues with nitric acid for the determination of trace elements by atomic spectrometry. *Analyst*. 1993; 118(7): 821-825.
  25. Pearson GF, Greenway GM. Recent developments in manganese speciation. *Trends Anal Chem*. 2005; 24(9): 803-809.
  26. Baluchnejadmojarad T, Roghani M. Chronic oral epigallocatechin-gallate alleviates streptozotocin-induced diabetic neuropathic hyperalgesia in rat: involvement of oxidative stress. *Iran. J Pharm Res*. 2012; 11 (4): 1243-1253.
  27. Yang In Kim, Heung Sik Na, Jung Soo Han, and Seung Kil Hong. Critical role of the capsaicin-sensitive nerve fibers in the development of the causalgic symptoms produced by transecting some but not all of the nerves innervating the rat tail. *J Neurosci*. 1995; 75(6): 4133-4139.
  28. Takeda A. Manganese action in brain function: Review. *Brain Res Brain Res Rev*. 2003; 41(1): 79-87.
  29. Santamaria AB. Manganese exposure, essentiality & toxicity. *Indian J Med Res*. 2008; 128(4): 484-500.
  30. Reaney SH, Bench G, Smith DR. Brain accumulation and toxicity of Mn(ii) and Mn(iii) exposures. *Toxicol Sci*. 2006 Sep; 93(1):114-124.
  31. Elder A, Gelein R, Silva V, Feikert T, Opanashuk L, Carter J, et al. Translocation of inhaled ultrafine manganese oxide particles to the central nervous system. *Environ Health Perspect*. 2006; 114(8): 1172-1178.
  32. Brenneman KA, Wong BA, Buccellato MA, Costa ER, Gross EA, Dorman DC. Direct olfactory transport of inhaled manganese ((54)MnCl(2)) to the rat brain: toxicokinetic investigations in a unilateral nasal occlusion model. *Toxicol Appl Pharmacol*. 2000; 169(3): 238-248.
  33. Gu L, Fang RH, Sailor MJ, Park JH. In Vivo clearance and toxicity of monodisperse iron oxide nanocrystals. *ACS Nano*. 2012; 6(6): 4947-4954.
  34. Sharma HS, Sharma A. Breakdown of the blood-brain barrier in stress alters cognitive dysfunction and induced brain pathology, new perspective for neuroprotective strategies. In: Michel Ritsner, editor., *Brain Protection in Schizophrenia, Mood and Cognitive Disorders*, Volume 1. Netherlands:

- Springer; 2010. p. 243-304.
35. Gallez B, Demeure R, Baudelet C, Abdelouahab N, Beghein N, Jordan B, et al. Non invasive quantification of manganese deposits in the rat brain by local measurement of NMR proton T1 relaxation times. *Neurotoxicology*. 2001; 22(3): 387-392.
36. Takeda A, Sawashita J, Okada S. Localization in rat brain of the trace metals, zinc and manganese, after intracerebroventricular injection. *Brain Res*. 1994; 658(1-2): 252-254.
37. Amrite AC, Kompella UB. Size-dependent disposition of nanoparticles and microparticles following subconjunctival administration. *J Pharm Pharmacol*. 2005; 57(12): 1555-1563.
38. Balasubramanian SK, Jittiwat J, Manikandan J, Ong CN, Yu LE, Ong WY. Biodistribution of gold nanoparticles and gene expression changes in the liver and spleen after intravenous administration in rats. *Biomaterials*. 2010; 31(8): 2034-2042.
39. Warheit DB, Hoke RA, Finlay C, Donner EM, Reed KL, Sayes CM. Development of a base set of toxicity tests using ultrafine TiO<sub>2</sub> particles as a component of nanoparticle risk management. *Toxicol Lett*. 2007; 171(3): 99-110.
40. Szalay B, Tátrai E, Nyíró G, Vezér T, Dura G. Potential toxic effects of iron oxide nanoparticles in in vivo and in vitro experiments. *J Appl Toxicol*. 2012; 32(6): 446-453.
41. Brieger K, Schiavone S, Miller FJ Jr, Krause KH. Reactive oxygen species: from health to disease. *Swiss Med Wkly*. 2012; 142: w13659. Available from URL: doi:10.4414/smw.2012.13659
42. Stefanescu DM, Khoshnan A, Patterson PH, Hering JG. Neurotoxicity of manganese oxide nanomaterials. *J Nanopart Res*. 2009; 11(8): 1957-1969.
43. van Rijn RM, Brissett DI, Whistler JL. Emergence of functional spinal delta opioid receptors after chronic ethanol exposure. *Biol Psychiatry*. 2012; 71(3): 232-238.
44. Yin QQ, Wu L, Gou ML, Qian ZY, Zhang WS, Liu J. Long-lasting infiltration anaesthesia by lidocaine-loaded biodegradable nanoparticles in hydrogel in rats. *Acta Anaesthesiol Scand*. 2009; 53(9): 1207-1213.
45. Ahmadi A, Khalili M, Mihandoust F, Barghi L. Synthesis and determination of acute and chronic pain activities of 1-[1-(3-methylphenyl) (tetralyl)]piperidine as a new derivative of phencyclidine via tail immersion and formalin tests. *Arzneimittelforschung*. 2010; 60(1): 30-5.
46. Fernandes A, Brites D. Contribution of inflammatory processes to nerve cell toxicity by bilirubin and efficacy of potential therapeutic agents. *Curr Pharm Des*. 2009; 15(25): 2915-2926.
47. Bird ED, Anton AH, Bullock B. The effect of manganese inhalation on basal ganglia dopamine concentration in rhesus monkey. *Neurotoxicology*. 1984; 5(1): 59-65.
48. Wang J, Rahman MF, Duhart HM, Newport GD, Patterson TA, Murdock RC, et al. Expression changes of dopaminergic system-related genes in PC12 cells induced by manganese, silver, or copper nanoparticles. *Neurotoxicology*. 2009; 30(6): 926-933.
49. Liu QS, Qiao JT, Dafny N. D2 dopamine receptor involvement in spinal dopamine-produced antinociception. *Life Sci*. 1992; 51(19): 1485-1492.
50. Barasi S, Ben-Sreti MM, Clatworthy AL, Duggal KN, Gonzalez JP, Robertson J, et al. Dopamine receptor-mediated spinal antinociception in the normal and haloperidol pretreated rat: effects of sulpiride and SCH 23390. *Br J Pharmacol*. 1987; 90(1): 15-22.
51. Gao X, Xin BM, Zhu CB, Wu GC, Xu SF. Effect of intrathecal injection of dopamine receptor agonists/antagonists on pain and acupuncture analgesia in rats. *Sheng Li Xue Bao*. 1998; 50(1): 43-48.
52. Greco R, Tassorelli C, Armentero MT, Sandrini G, Nappi G, et al. Role of central dopaminergic circuitry in pain processing and nitroglycerin-induced hyperalgesia. *Brain Res*. 2008; 1238: 215-223.
53. Borsook D, Upadhyay J, Chudler EH, Becerra L. A key role of the basal ganglia in pain and analgesia - insights gained through human functional imaging. *Mol Pain*. 2010; 6: 27.
54. Wang J, Liu Y, Jiao F, Lao F, Li W, Gu Y, et al. Time-dependent translocation and potential impairment on central nervous system by intranasally instilled TiO<sub>2</sub> nanoparticles. *Toxicology*. 2008; 254(1-2): 82-90.
55. Sárközi L, Horváth E, Kónya Z, Kiricsi I, Szalay B, Vezér T, et al. Subacute intratracheal exposure of rats to

- manganese nanoparticles: behavioral, electrophysiological, and general toxicological effects. *Inhal Toxicol.* 2009; 21 Suppl 1: 83-91.
56. Hudspith MJ, Harrison S, Smith G, Bountra C, Elliot PJ, Birch PJ, Hunt SP, Munglani R. Effect of post-injury NMDA antagonist treatment on long-term Fos expression and hyperalgesia in a model of chronic neuropathic pain. *Brain Res.* 1999; 822(1-2): 220-227.

Archive of SID